
WAVELETGPT: WAVELET INSPIRED LARGE LANGUAGE MODELS

Prateek Verma

Stanford Natural Language Processing Group*
Department of Computer Science
Stanford University
Stanford, CA, 94305
prateekv@cs.stanford.edu

ABSTRACT

Large Language Models (LLMs) have ushered in a new wave of artificial intelligence advancements impacting every scientific field and discipline. We live in a world where the data around us, e.g., text, audio, and music, has a multi-scale structure associated with it. This paper infuses LLMs with a traditional signal processing idea, wavelets, during pre-training to take advantage of the structure. Without adding **any extra parameters** to a GPT-style LLM architecture in academic setup, we achieve the same pre-training performance almost twice as fast in text, raw audio, and symbolic music. This is achieved by imposing a structure on intermediate embeddings. When trained for the same number of training steps, we achieve significant gains in performance, comparable to pre-training a larger neural architecture. Our architecture allows every next token prediction, access to intermediate embeddings at different temporal resolutions in every layer. This work will hopefully pave the way for incorporating multi-rate signal processing ideas into traditional LLM pre-training. Further, we showcase pushing model performance by improving internal structure instead of just going after scale.¹

1 INTRODUCTION AND RELATED WORK

LLMs have ushered in a super-renaissance of AI advancements and are touching every scientific and engineering discipline. At the heart of this is the Transformer architecture (Vaswani et al., 2017), initially proposed for machine translation. Transformer architecture became the backbone of GPT (Generative Pretrained Transformer) language models (Brown et al., 2020) first proposed by Open-AI. Modern LLMs are trained on a straightforward objective: To predict the next token given the previous context, preserving the causality. This not only works for language but also for robotics (Brohan et al., 2023b;a), protein sequences (Madani et al., 2020), raw audio waveforms (Verma & Chafe, 2021), acoustic and music tokens (Huang et al., 2019; Verma & Smith, 2020; Borsos et al., 2023), videos (Yan et al., 2021) etc. This simple recipe of tokenization/creating an embedding and feeding it to transformers also has given rise to non-causal architectures such as BERT (Devlin et al., 2019), Vision Transformers (Dosovitskiy et al., 2021), Audio Transformers (Verma & Berger, 2021) and Video Transformers (Selva et al., 2023). The recent surge in multi-modal LLMs similar to Gemini family (Team et al., 2023) or Chameleon Chameleon (2024) would pave the way for computers able to reason like humans. With increased performance by scale, LLMs are reaching hundreds of billions of parameters (Brown et al., 2020), with Google’s Switch Transformer even reaching a trillion parameters (Fedus et al., 2022). Recent concerns suggest AI research is shifting from academia to industry, according to a Washington Post article by (Nix, 2024). This work aims to enhance LLM capabilities to match those of larger architectures or achieve equivalent performance in fewer training steps. We extract intermediate embeddings from each decoder block and impose a hierarchical multi-scale structure without adding parameters. The signals across tokens in the intermediate layers are extracted, which we modify, similar to wavelet decomposition, while maintaining causality (Figure 1).

¹* This work was carried out in early 2023 while Prateek Verma was with the Stanford Natural Language Processing Group in the Department of Computer Science at Stanford University.

Unlike previous techniques that enhance smaller models with larger ones, our approach focuses on improving performance during pre-training. A common approach is knowledge distillation (Hinton et al., 2015), where a larger model guides a smaller one. (Gu et al., 2024) used KL divergence to enhance next-token prediction from teacher model feedback, still relying on a powerful model rather than training the smaller one from scratch. A line of work, such as (Nawrot et al., 2022), proposed hierarchical transformers using upsampling-downsampling operations, similar to the hourglass U-Net architecture (Long et al., 2015) in computer vision. This approach achieves results comparable to those of Transformers but with more efficient computation. Clockwork RNN (Koutnik et al., 2014) improves long-context modelling by splitting RNN neurons into modules that update at different clock rates. Only a few modules activate at each time step, enabling efficient learning of long-term dependencies. In contrast, our approach modifies intermediate embeddings with simple tweaks without using separate learning modules or varying update rates. Model pruning (Sun et al., 2024) removes weights based on their salience to match the same performance as a large model like LLAMA (Touvron et al., 2023), with fewer compute flops during inference. However, this approach still relies on starting with a pre-trained large model rather than training from scratch. We also exclude quantization methods like Dettmers et al. (2024), which focus on improving inference or fine-tuning existing models. The other line of work is tinkering with the intermediate embeddings. Tamkin et. al (2020) proposed hand-tuned filters on the Discrete Cosine Transform- DCT over the entire context length (Ahmed et al., 1974) of the latent space for different NLP tasks for non-causal BERT (Devlin et al., 2019), making them not applicable for causal applications such as language modelling. There has been work on applying ideas from signal processing-like methods to BERT-like non-causal architectures. We discuss two here, FNet and WavSPA. They focus on improving attention, which is different from our work on GPT, which retains a vanilla attention layer. FNet proposed by Lee-Thorp et al. (2022) removes the costly attention mechanism, replacing it with a 2-D FFT block. This operation is non-causal as it looks into future tokens for computing 2-D FFT. WavSpA (Zhuang et al., 2024) carries attention mechanism in the wavelet space. Since the wavelet transform is a multi-resolution, capturing long-term dependencies at various time scales, the input sequences are transformed into wavelet space, and the attention mechanism is carried out and then reconstructed. However, computing wavelet transform is non-causal, making them non-applicable for GPT-based LLMs as they look at the entire sequence length for capturing variations from coarsest to finest scales (as can be seen in Figure 1 of (Zhuang et al., 2024)). This paper modifies only the intermediate embeddings of a LLM model. Our work is inspired by neuroscience, which provides evidence that the human brain learns multi-scale representations for language at multiple time scales (Caucheteux et al., 2023) instead of fixed-resolution representations. Our paper explicitly imposes multi-scale representation onto every intermediate decoder embedding at different dimensions. The contribution of the paper is as follows: 1) We propose, to the best of our knowledge, the first instance of incorporating wavelets into LLM pre-training. We add multi-scale filters onto each of the intermediate embeddings of decoder layers using the Haar/learnable wavelet pipeline. This allows every next token prediction access to multi-scale intermediate embeddings in every decoder layer instead of fixed-resolution representations. 2) We show to speed the pre-training of a shrunk down GPT like transformer-based LLM in the range of 40-60%, with adding multi-scale structure. With the same number of training steps, the model gives performance boost, akin to adding several layers.

2 DATASET

We use four open-source datasets from four different domains for seeing how well we do for next token prediction: natural language, symbolic music, speech tokens, and raw audio waveform. For text, we choose text-8 (Mikolov et al., 2012). We choose this over other datasets as i)it is a famous and widely cited character-level language modelling dataset, and ii) it uses a simple vocabulary (space + 26 lowercase characters) to detach the effects of various tokenizers. It has 100M characters with split training split as given by Al-Rfou et al. (2019). For raw audio, the goal is to predict the next sample given the context. We use the YouTube-Mix-8 dataset for long-context modeling (Goel et al., 2022; Verma, 2022). Our vocabulary size is 256, with a sampling rate of 16KHz as input is 8-bit. We use a third dataset, MAESTRO (Hawthorne et al., 2019), containing over 1000 MIDI files of classical music pieces. We use the tokenizer proposed by Huang et al. (2019), which converts MIDI tracks into discrete tokens with a vocabulary size 388. Finally we use 1000 hours of LibriSpeech dataset and a widely used ENCODEC Défossez et al. (2022) tokenizer in setup similar to VALL-E Wang et al. (2023) to model acoustic tokens. The goal in this work, is how well we can model the coarsest tokens, as errors in modeling the coarser tokens will lead to the finer tokens being modeled

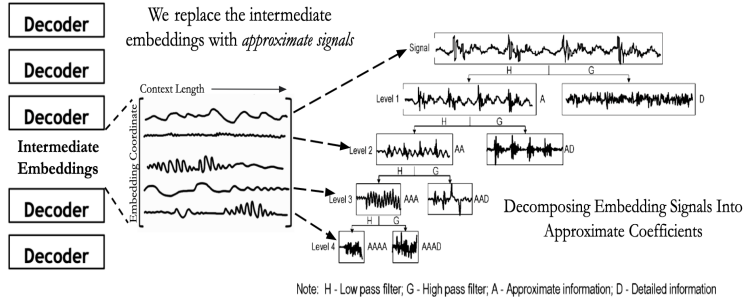


Figure 1: Manipulating signals in between decoder blocks of GPT. We compute a 1-D causal discrete haar wavelet transform or learnable approximation at different levels to mimic the multi-scale structure for text, raw audio, and symbolic music for each signal. The one on the right is from Gao & Yan (2006), which gives a detailed account of non-stationary signal processing for 1-D signals. We take the leftmost route of approximate coefficients, which allows us to coarsest to the finest scales.

incorrectly as they are conditioned on the coarsest token, thus affecting model performance. The goal in all four modalities is not to chase state-of-the-art performance, as *this paper was written in an academic setting with very few computational resources*. We report how well the model performs in pre-training instead of post-training, as we are interested in building better foundational architectures in this paper. We push the capabilities of smaller decoder architectures that can be trained in academia. We compare pre-training performance to the shrunk-down version of GPT with/without adding a multi-scale structure to the embeddings using Haar or learnable kernels.

3 METHODOLOGY

This section will describe the approach to incorporating wavelets into transformer-based Large Language Models while retaining the causality assumption. The ideas described here are generic and can be easily extrapolated to setups without a Transformer architecture, e.g. state space architectures. For any signal, we compute a version of the discrete wavelet transform and incorporate it back into the signal. Let $x_{(i)}^l$ be the output of the l^{th} decoder layer, representing the activation along the i^{th} coordinate, with a dimension equal to the context length L of the transformer-based GPT model. In the original GPT architecture with $N + 1$ layers and embedding dimension E , we obtain $N \cdot E$ signals of length L from intermediate embeddings between decoder blocks, where E ranges from $[0 - 128)$ dimensions. A wavelet is a signal with zero mean and non-zero norm designed to address the limitations of traditional Fourier-based representation. For any signal $x[n]$, the discrete wavelet transform resembles passing the signal through filters of varying resolutions, as illustrated in Figure 2. We will use the Haar wavelet, a family of square-shaped functions this paper obtained from a mother wavelet via scaling and shifting operations. Given a mother wavelet function ψ , we develop the child wavelets as $\psi_{j,k}[n]$, where j is the scaling factor and k is the shift factor.

$$\psi_{j,k}[n] = \frac{1}{\sqrt{2^j}} \psi \left(\frac{n - k2^j}{2^j} \right) \quad (1)$$

These signals are shifted and scaled to capture information at various time scales, with n representing time or the context length. This concept resembles the diagram in Figure 1, which illustrates capturing different signals in the intermediate layers of Transformer decoders at various resolutions. We now define the discrete wavelet transform, which passes any signal through filters and downsampling operations. This process, shown in Figure 2, is similar to a convolutional neural network (CNN) like ResNet (He et. al, 2016), featuring learned convolutional filters analogous to $h[n]$ and $g[n]$, along with downsampling, such as max pooling. In traditional convolutional architectures, we typically follow one branch of Figure 2, recursively taking the output of filters and downsampling. This similarity contributed to the popularity of wavelets in the 1990s and 2000s for image understanding, reflecting parallels with convolutional architectures (Huang & Aviyente, 2008; Kingsbury & Magarey, 1998). As we use Haar wavelets, this involves passing the signal through low-pass and high-pass

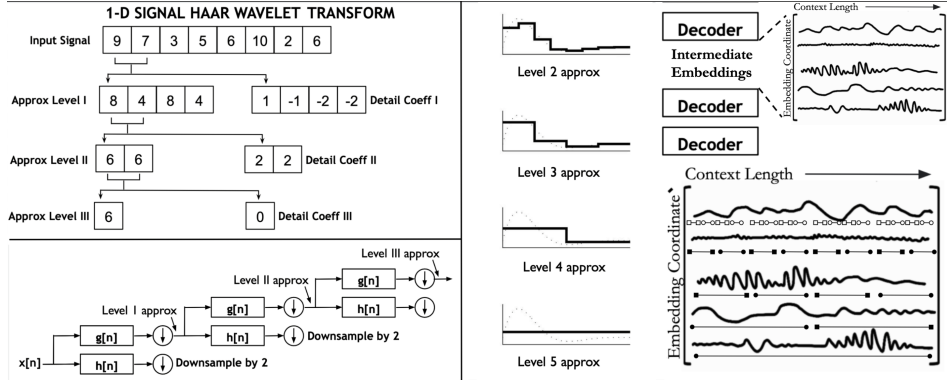


Figure 2: (Bottom L): A 3-level filter bank tree generates signals at different resolutions. Approximate coefficients are computed by applying a wavelet’s impulse response & recursively down-sampling.(Top L): Approximate and detailed coefficients are iteratively calculated via first-order averages/differences and down-sampling until a single scalar represents the signal.(R): For a 32-length signal, Haar wavelet captures coarsest to finest approximations, is redrawn from (Flores-Mangas, 2014). Embeddings evolve at different rates via causal wavelet approximation, with coarse (level 5) and fine (level 2) resolutions, embedding multi-scale information into decoder layers for every token.

filters corresponding to the kernels $g[n]$ and $h[n]$. The Haar wavelet transform averages and computes differences, with impulse responses $g[n] = [\frac{1}{2}, \frac{1}{2}]$ and $h[n] = [\frac{1}{2}, -\frac{1}{2}]$. Figure 2 provides a detailed explanation of the discrete wavelet transform. For a 1-D signal $x[n]$ of length L , we obtain level 1 coefficients by applying filters $g[n]$ and $h[n]$, followed by downsampling. Thus, the approximation coefficients y_{approx} and y_{detail} result from an LTI system defined by convolution followed by downsampling by two, as seen in Equation 2. This behaviour is reflected in Algorithm 1.

$$y_{approx}[n] = \sum_{k=-\infty}^{\infty} x[k]g[2n - k] \quad ; \quad y_{detail}[n] = \sum_{k=-\infty}^{\infty} x[k]h[2n - k] \quad (2)$$

To obtain multi-scale representations of the original signal, the operation for $x[n]$ is recursively applied to y_a (approx) to derive level 2 wavelet coefficients y_a^2 and y_d^2 (detail). Here, $x[n]$ represents intermediate signals across the context length at each decoder block output in the LLM. The approximate coefficients y_a and y_d , along with their decompositions $\{y_a, y_d, y_a^2, y_a^3, y_a^4, \dots\}$, are used for further processing. Notably, y_a^2, y_a^3, y_a^4 have lengths reduced by factors of 2, 4, 8, \dots . The Haar wavelet transform averages adjacent samples while preserving causality by averaging current and past samples. Higher-order coefficients capture averages over larger context lengths, as shown in Figure 2. We can continue until only a single scalar value remains, representing the mean of the signal. The Haar wavelet transform computes averages and differences to create a multi-resolution representation, capturing low and high frequencies at different resolutions. Figure 2 illustrates the same signal captured at coarser and finer representations using Haar wavelets, applied to intermediate embeddings, allowing each next token prediction access to these representations. For the case of learnable wavelet kernels, we create a multi-resolution representation by varying the kernel size (Algorithm 1) to allow the LLM to learn the optimal kernels optimized for the next token prediction.

3.1 CONNECTING WAVELETS AND LLM EMBEDDINGS

In many signal processing applications, first-order detail and approximate coefficients help understand signals at various levels. We aim to do the same with signals from intermediate transformer embeddings across tokens. However, we focus only on approximate coefficients. Our premise is that real-world data is structured—text ranges from letters to words, sentences, and topics, while symbolic music ranges from notes to motifs and pieces. Using the Haar wavelet, this can be approximated as a simple averaging operation, as described earlier. For the learnable version, we allow weights of the kernel for the multi-scale version to be optimized according to how best we can predict the next token. Continuing with the approximate coefficients will eventually yield a single scalar, the average of the

entire signal in the case of the Haar wavelet. Several methods can be employed to match the original signal’s sequence length from the approximation coefficients, including up-sampling. For clarity, we refer to the signal approximated at a specific level with the same length as the “approximate signal” at that level, distinguishing it from the shorter approximate coefficients. In Figure 2 (R), to obtain the signal approximation at various levels matching the original input signal $x[n]$, we apply the wavelet kernel by multiplying the approximate coefficients with the kernel for that level (e.g., $[1, 1]$, $[1, 1, 1, 1]$, etc.). This is illustrated in the piecewise constant function shown in Figure 2. Different LLM embedding coordinates define unique resolution kernels, each corresponding to a specific scale for data capture. The reconstructed signal $x_{\text{recon}}[n]$, a method to derive the “approximate signal”, is computed from wavelet coefficients c_j at level j as:

$$x_{\text{recon}}^j[n] = \sum_k c_k \cdot \psi_{j,k}[n] \quad (3)$$

Equation 3 requires storing child wavelets at various approximations, complicating the process and rendering it non-causal as computing c_k considers the entire signal. Due to the dependence of c_k on future information, we cannot use this to reconstruct the signal from its approximate coefficients. To adapt this for LLM, we simplify the computation of the “approximate signal” in a differentiable manner using a variant of the equation from Equation 3 in both multi-resolution learnable/non-learnable kernel settings. For the Haar wavelet, we compute an average of the input signal with varying kernel lengths, increasing the length until it approximates the entire signal. The kernel length determines the level of signal approximation. LLMs operate under a causality assumption, modifying the signal at a location using prior samples within the kernel length. We zero-pad the signal to the left when the window length is shorter than the kernel. Wavelet transform at different levels gives several versions of the signal at different resolutions, which can mess up the structure of the intermediate Transformer embeddings. We create different resolutions for signal approximations parameterized by the embedding dimension to address this. In Section 4.4, we make these kernels learnable, allowing the architecture to maintain multi-scale operation (Equation 3), with learnable weights with $x_{\text{recon}}[n]$ now being learned. The resolution is parameterized by the embedding coordinate, as described next.

Algorithm 1 Wavelet-GPT

E : Model or Embedding Dimension
 L : Context Length
 $N + 1$: Number of Decoder Layers
for layer $l = 1, 2, \dots, N$ **do**
 $\mathbf{x}^l \leftarrow$ Output of Transformer l^{th} Decoder Block //Dimension $E \times L$
 $\mathbf{xn}^l \leftarrow$ Modified Transformer Embedding Replacing \mathbf{x}^l
 $\mathbf{xn}_{(i)}^l \leftarrow \mathbf{x}_{(i)}^l$ For Embedding dimension $i < E/2$

 $\mathbf{f}(i) \leftarrow 2^F$ where //Finding kernel length function of embedding coordinate nearest power of 2
 $F = \text{int}(L_k * (i - E/2)/(E/2 - 1)) \quad L_k = \lfloor \log_2(L) \rfloor + 1 \quad i \geq E/2$

 $\mathbf{xn}_{(i)}^l(\mathbf{k}) \leftarrow \frac{1}{\mathbf{f}(i)} \sum_{\mathbf{m}=\mathbf{k}-\mathbf{f}(i)}^{\mathbf{k}} \mathbf{x}_{(i)}^l(\mathbf{m}) \quad i \geq E/2$ // For Non-learnable fixed Haar wavelet
 $\mathbf{xn}_{(i)}^l(\mathbf{k}) \leftarrow \sum_{\mathbf{m}=0}^{\mathbf{f}(i)-1} \mathbf{h}(\mathbf{m}) \cdot \mathbf{x}_{(i)}^l(\mathbf{k} - \mathbf{m}) \quad i \geq E/2$ // For learnable wavelet kernel h
end for

3.2 WAVELET COEFFICIENTS BY EMBEDDING DIMENSION COORDINATES

One option is to compute the *approximate signals* for each coordinate signal $x_{(i)}^l$ across all decoder layers at levels I to IX. For a context length of 512, this would require nine additional signals with resolutions of 512, 256, 128, 64, 32, 16, 8, 4, and 2, significantly increasing the architecture’s complexity and necessitating major modifications to our GPT model. We propose a novel solution to address this. Instead of computing all levels of *approximate signals* for every intermediate embedding dimension, we parameterize the level by the embedding dimension index. We want to steer the embeddings only a little into the inductive biases we impose to avoid too much tinkering with what they learn. Transformers have been wildly successful without incorporating any inductive biases. Ideally, we want the best of both worlds, nudging intermediate GPT embeddings in only half of the dimensions. We adjust intermediate GPT embeddings in only half the dimensions. Embeddings from $E/2$ to E (coordinates 64 to 128 when $E = 128$) remain unchanged. For the rest, we apply processing based on their index i . Mathematically, if $x^l(i)$ is an intermediate embedding after the l^{th}

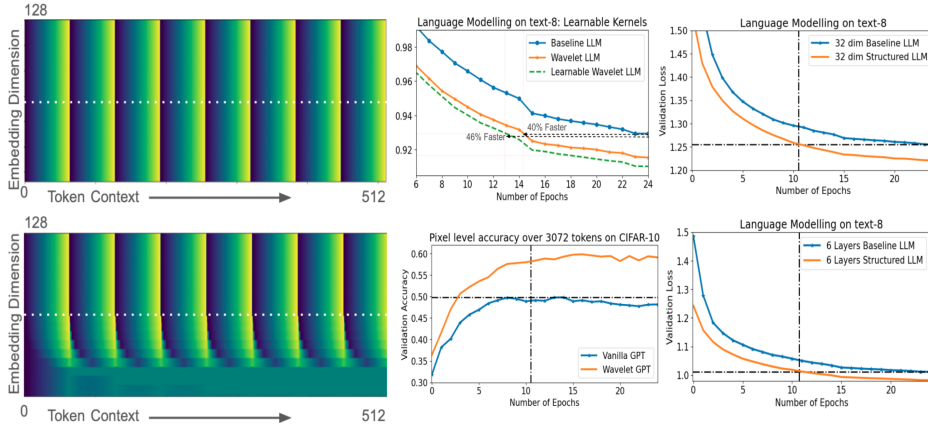


Figure 3: (Left) Toy example showing how variations in how embeddings move along a token dimension and how we impose multi-rate structure where different embedding dimensions advance at distinct rates while maintaining causality. Latent space now learns at varying rates for each token, with patterns dispersing from dimension 64 to 0. (Right) Validation loss during pre-training on text-8 with learnable multi-scale structure. The model achieves comparable performance nearly twice as fast. When trained for the same number of epochs, we get a performance boost akin to adding additional decoder layers. We also demonstrate the architecture’s performance on text-8 with a 32-dim model, matching the speedup similar to that seen for a 128-dim model and a shallower six layers. For the LRA image benchmark, we observe a 10% performance increase without adding extra parameters.

decoder layer along the i^{th} dimension, the modified signal $xn^l(i)$ equals $x^l_{(i)}$ for $i \in [E/2, E]$. For $0 \leq i < E/2$, we impose structure using an approximate signal calculated from wavelet coefficients corresponding to the index i . We use a mapping function f that takes coordinate i (ranging from 0 to $E/2$) and returns the kernel size corresponding to approximation levels from I to IX . The linear function gradually increases from level I (kernel size two at $i = 0$) to level IX (kernel size 512 at $i = E/2$, or the coarsest representation for a generic case, i.e., a scalar). Now, let us find out how we compute the modified new signal $xn^l_{(i)}$ that replaces the original intermediate Transformer embeddings $x^l_{(i)}$. $f(i)$ denotes the kernel size for the coordinate i . Now, the modified signal is:

$$xn^l_{(i)} = x^l_{(i)} \text{ for } i > E/2 \quad ; \quad xn^l_{(i)}(k) = \frac{1}{f(i)} \sum_{m=k-f(i)}^k x^l_{(i)}(m). \quad (4)$$

For cases where $k - f(i) < 0$, we zero-pad the signal to ensure valid average/kernel computation. Specifically, for the Haar wavelet, the modified signal acts as a causal moving average filter with finite length, averaging the embedding signal along the i^{th} coordinate with a kernel size determined by $f(i)$. This operation does not introduce new parameters, maintain causality in LLMs, and prevent future token leakage, as seen in Equation 4. We can extend this approach to learn an optimal kernel specific to the task. In Algorithm 1, each value of the modified signal at token k is computed using a convolution with a learned kernel $h(\cdot)$ and variable length $f(i)$, parameterized by the embedding coordinate dimension i . Each kernel is learned independently for every signal in LLM.

3.3 IMPOSING STRUCTURE: TOY EXAMPLE

In Figure 3, we illustrate a toy example of how we impose structure onto decoder Transformer embeddings. The left side shows eight variations along the token dimension, with onset/sudden bursts at token indices 32, 64, etc., decreasing to zero before rising again. As discussed in the introduction, datasets inherently possess a hierarchical structure, which we capture by imposing intermediate Transformer embeddings at each layer. In this example, we retain embeddings at the original resolution for half the dimensions (split by a white line). For the other half, we gradually increase the kernel length across the context and compute the average causally. The final embedding

dimension averages over the token dimension with a kernel size equal to the context length (zero-padding if necessary). This creates highways, allowing embeddings to move at different rates: the coordinates from $E/2$ to E move at the Transformer’s original speed, while those from 0 to $E/2$ transition from faster to slower movement. This approach enables the attention mechanism to utilize multi-scale features at varying rates across all layers and tokens, as explored in the next section. Further, this multi-scale structure can be made learnable, driven by just the next token prediction.

4 EXPERIMENTS

We explain how we incorporated the idea of infusing wavelets into a large language model pre-training. All of the models are trained from scratch, which requires substantial computing. The main aim of these experiments is to show how the performance of the models across four modalities improves with/without doing intermediate modifications on embeddings. We also benchmark on LRA tasks. Training modern millions of parameter architecture beyond anything that can be trained from scratch in an academic setup with limited compute resources. Hence, we first proposed a shrunk-down baseline architecture. We only report how well our generative model does are only interested in quantifying the likelihood scores for the generative architecture pre-training similar to papers such as Mega-Byte Yu et al. (2023) and Music Transformer Huang et al. (2019) that only report NLL scores in the entire paper. We also are improving the core Transformer block, report on LRA benchmarks. Our experiments, based on the GPT-2 architecture, feature a stack of 10 Transformer decoder layers with a context length of 512, trained from scratch. Each modality—text, symbolic music, and raw waveform—shares the same architecture, using an embedding dimension of 128, a feed-forward dimension of 512, and 8 attention heads. We implement a two-layer feed-forward MLP present in Transformer, each layer matching the feed-forward dimension, rather than the single layer typical in Vaswani et al. (2017) for both our baseline and proposed architecture. The final decoder outputs to a dense layer of 2048 neurons, followed by a layer matching the vocabulary size: 27 for text8, 256 for raw waveform (Goel et al., 2022; Verma, 2022), 388 for symbolic music, and 1024 for ENCODEC speech tokens. Baseline models consist of standard Transformer decoder blocks without modified embeddings. We retain half of the embedding coordinates for our proposed architecture and impose either a fixed or learnable multi-scale structure on the other half for all intermediate layers. We do not compare against larger architectures, as this paper focuses on pre-training from scratch. Instead, we present a scaled-down version of GPT-2 suitable for resource-limited academia, evaluating pre-training performance with and without wavelet-inspired blocks. All models were trained from scratch in TensorFlow Abadi et al. (2016) for 25 epochs, starting with a learning rate of $3e-4$, decreasing to $1e-5$ when loss plateaued. Each model utilized 1M training points, totalling 500 million tokens, randomly cropped from the dataset. The MLP, attention layers use a dropout of 0.1 with no extra regularization. We measured performance using negative log-likelihood loss, as this method improves the core architecture of the transformer-based GPT - helping achieve the objective we want to achieve: predict the next token correctly. Since we are operating on intermediate embeddings, our work can hopefully generalize to setups with structured data similar to text, raw audio, and symbolic music, where one can go from a fine-grained structure to a coarse structure. As seen in Figure 3, we can impose a multi-scale structure that allows the attention mechanism to learn dependencies across various embeddings and inject some information that can capture coarse and fine-grained structures into embedding coordinates.

4.1 PERFORMANCE ON MODALITIES

We compared the performance of our baseline architecture across three modalities—text, symbolic music, and audio waveform—with and without wavelet-based intermediate operations. Results showed significant performance improvements in all modalities with the same number of training steps. To illustrate, a 0.04 decrease in validation loss is comparable to going from a 16 to a 64-layer model on text-8 dataset (papers-with code, 2024). As shown in Figure 4, our modified GPT architecture achieves this loss nearly twice as quickly in training steps as the original model, showing that GPT-like architecture can take advantage of the structure we imposed on half of the embedding dimensions. This speedup, i.e., the number of epochs/steps taken to achieve the same performance (SP: same performance epoch), is even smaller for raw audio due to the quasi-stationary nature of audio signals at smaller time scales (20-30 ms for harmonic sounds). For a sampling rate of 16KHz, a context length of 512 would correspond to 32ms, which may be one of the reasons that some of the coordinates nail down the contents of the context in fewer coordinates onto which we impose structure. The convergence is significantly faster for the raw waveform LLM setup and achieves nearly twice

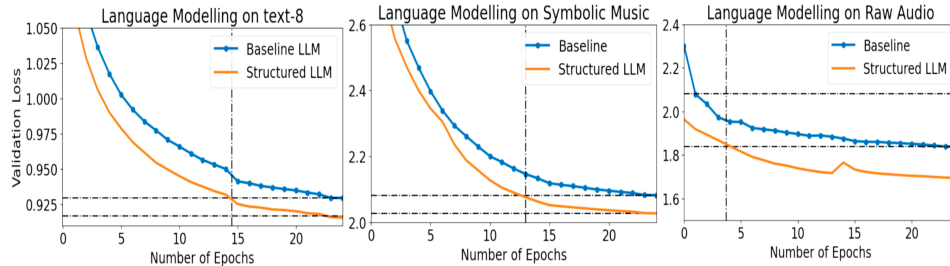


Figure 4: Results for three modalities: natural language, symbolic music, and raw audio. We achieve much faster performance than the baseline, almost twice as fast on shrunk-down GPT-like architecture. When trained for the same number of epochs, we see a substantial improvement in the pre-training performance, equivalent to a much larger architecture. The black vertical line denotes the epoch at which our architecture achieves the same performance as our baseline architecture.

the speed of text-8 and symbolic music. We also ran benchmarks on LibriSpeech corpus on speech and acoustic tokens, further strengthening our claims that our method is generic enough to handle several different types and modalities of tokens. Finally we run our method on audio classification with Audio Transformer over 200 categories of audio for FSD-50K benchmarks Fonseca et. al (2020). We not only get a performance boost but also get speedups, thereby showcasing the ubiquity of our proposed method not only for generative modelling but for classification as well.² We also compare the absolute clock run times of our modifications in both learnable/non-learnable setups. Table 1 reports the time taken to complete one epoch relative to our baseline architecture. Our method is computationally inexpensive, as it primarily involves fixed kernel multiplication or learning a single filter convolutional kernel with variable context lengths across different embedding dimensions.

Table 1: Comparison of the negative-log likelihood (NLL) scores for our architecture with three modalities with/without adding wavelet-based hierarchical structure and learnable wavelet transform.

Modality	Baseline	Proposed	SP Epoch	SpeedUp	Rel. GPU Hrs
Text-8	0.93	0.92	14.5 epochs	42%	1.013
Raw Audio	1.84	1.70	3.7 epochs	85%	1.042
Symbolic Music	2.08	2.02	13 epochs	48%	1.059
Text-8 (Learnable)	0.93	0.91	12.9 epochs	48.4%	1.094
Wiki-103 (Learnable)	4.11	4.05	9.5 epochs	62%	1.130
LibriSpeech (Learnable)	2.43	2.40	9.2 epochs	63.2%	1.110
FSD-50K	40.6%	42.8%	32/92 epochs	65.2%	1.037

4.2 AUDIO CLASSIFICATION BENCHMARK

We explore the strength of our method for a typical audio classification on a standard audio classification benchmark FSD-50K. The goal is to correctly identify the categories of sound present in 1s of audio. For this we use a transformer based architecture similar to Audio Transformer as our baseline model. It consists of 128 convolutional filters with length 200 learned over 25ms of audio sampled at 16KHz yielding patches of 400 length audio samples. The convolutional filter output is then max-pooled across the 25ms window to give a single vector of length 128 i.e. the number of convolutional filters being fed to a Transformer stack of 6 layers with model dimension as 64 similar to Verma & Berger (2021). We reported on the top-5 % accuracy and relative gain in mAP scores for our proposed baseline architecture and manipulating intermediate embeddings with learnable/non-learnable kernels. We see that we get a performance boost of about 2% and a faster convergence of more than 60% as reported in Table 1. We add the results of our experiments in the figure below for learnable version, fixed kernels and baseline.

²We have further explained this in Appendix

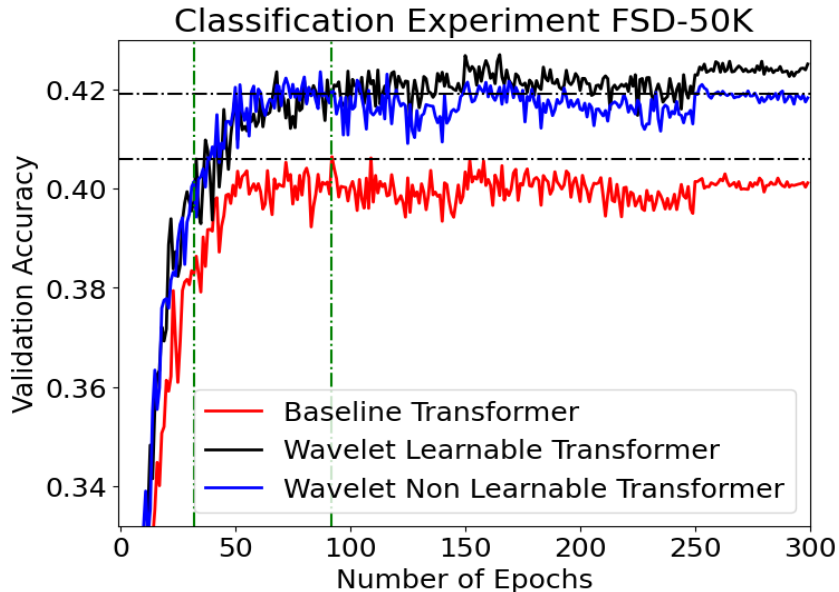


Figure 5: Results for FSD-50K using Audio Transformer top-5 accuracy for baseline, learnable and fixed kernels. Notice the two vertical green lines showing the top accuracy reached and then the same accuracy reach with our proposed transformer 60% faster with addition of no extra parameters.

4.3 SIMILARITIES AND DIFFERENCES WITH EMA

We compare with Exponential Moving Averages (EMA) on intermediate signals. Unlike the Haar wavelet, which takes fixed window weights, which takes the mean of the signal in the window, EMA uses an exponential kernel. Let the signal $x_i^l(t)$, after the l^{th} layer, be of length equal to context length, with t being the token index from 0 to L at embedding dimension i . The modified signal s_t is:

$$s_0 = x_i^l(0) \quad s_t = \alpha x_i^l(t) + (1 - \alpha)s_{t-1}$$

where α , the decay factor, satisfies $0 < \alpha < 1$. Unlike an EMA, our method uses a finite kernel, with zero weights outside a specified length, capturing multi-scale information. In text-8 experiments, we applied EMA on half of the embedding dimensions, with α linearly varying between 0 and 1 for dimensions 64 to 128. This under-performed compared to our baseline, with an NLL score of 0.94, while our baseline and proposed method achieved scores of 0.93, 0.92, and 0.91 for non-learnable and learnable cases, respectively. Our method provides a simple, signal processing-based scheme that optimizes weights across multiple resolutions driven by next-token prediction and outperforms EMA. Depending on α , the EMA filter produces an exponential kernel while we maintain a constant kernel or allow weights learned from scratch optimized for the next token prediction. Further, EMA is an Infinite-Impulse Response (IIR) filter, whereas the Haar wavelet-based kernel is a Finite Impulse Response (FIR) filter. Consequently, for each value update, the contributions from previous samples never reach zero. These can accumulate significantly at longer context lengths for certain α . The recursive, non-learnable nature of the EMA IIR filter ensures some contribution from all embeddings, which explaining performance degradation. In contrast, our method uses zero weights outside the kernel length, effectively capturing multi-scale information, explained more in Appendix.

4.4 EFFECT OF DEPTH AND MODEL DIMENSION

We explore two variants of our architecture for experiments on text-8 – i) reducing model dimension from 128 to 32 and ii) reducing the number of layers. The model with dimension 32 for a 10-layer Transformer decoder architecture with eight heads still retains faster performance as a baseline, almost twice as fast as seen in Figure 4, and achieves the performance without doing the modification (as seen as a baseline) around ten epochs. We retain the exact architecture reported in Table 1 for the

second experiment. We have 6 Transformer Decoder layers, keeping the rest of the parameters the same (feed-forward dimension four times that of the model dimension, eight attention heads) to see the effect of depth. The model, with Haar-inspired modifications, similar to Table 1 results, continues to get the same performance as the baseline twice as fast, as seen in Figure 3.

4.5 MAKING MULTI-SCALE KERNELS LEARNABLE

We allow each of the kernels to be learnable. In the previous section, we defined the shape of the kernel and computed approximate signals of intermediate layer activations across all layers, with different resolutions occurring at different embedding dimensions to mimic a causal version of the wavelet transform. Now, we allow each kernel of length L at a particular level to be learnable for computing the *approximate signal* for various resolutions, yet another way to compute it. By making the computation of approximate signal learnable, the model can learn how to weight every decoder layer dimension instead of putting a fixed kernel, e.g. exponentially weighted average. This, as can be seen, Algorithm 1 only allows 20k or 0.2 % extra parameters to our base decoder architecture. This further improves our performance from 42% to 48% faster speedup to get a similar baseline performance, seen in Figure 4, carried out on the text-8. We also benchmark on Wiki-103 to demonstrate that our method works with the GPT-2 tokenizer. As shown in Table 1, we match the performance of a 10-layer architecture at more than twice the speed. In addition to faster convergence, we see a 3.6-point improvement in perplexity scores over the baseline model. Our architecture, with a 512 context length and 128 model dimensions, is a simplified version of GPT-2/3, constrained by academic resources. Section 4.4 scales with model size, highlighting the potential for future improvements for decoder-only LLM architectures across modalities and datasets.

5 LONG RANGE ARENA BENCHMARKS

We adapt our architecture for Long-Range Arena (LRA) tasks Tay et al. (2021), which test models on long-range prediction across text, images, and mathematical expressions. These tasks evaluate the model’s ability to handle similarity, structure, and reasoning over extended contexts. We focus on transformer-based architectures, as recently reported by Liu et al. (2024), while other variants include state-space and hybrid models or tweaking attention mechanisms. For text, we perform binary classification on the IMDb review dataset (Maas et al., 2011) using byte-level data with a context length of 2048 to determine if a movie review is positive or negative. We use CIFAR-10 from the LRA benchmark for images, classifying sequences of 3072 pixels into one of ten categories. Lastly, we benchmark on Long ListOps, testing the model’s ability to understand hierarchically structured data in extended contexts. As per LRA paper Tay et al. (2021), ”The dataset is comprised of sequences with a hierarchical structure and operators MAX, MEAN, MEDIAN and SUM_MOD that are enclosed by delimiters (brackets). An example (much shorter) sequence is as follows: **INPUT:** [MAX 4 3 [MIN 2 3] 1 0 [MEDIAN 1 5 8 9, 2]] **OUTPUT:** 5. In our task, we use a version of ListOps of sequence lengths of up to 2K to test the ability to reason hierarchically while handling long contexts. In the above example, the model needs to access all tokens and model the logical structure of the inputs to make a prediction. The task is a ten-way classification task and is considerably challenging.” We use the setup provided by Khalitov et al. (2022) to extract the data and be uniform with other benchmarks. We use a nearly identical architecture for all three modalities, only modifying the embedding matrix to accommodate different tokenizers and output categories. Our baseline consists of a 6-layer causal Transformer decoder with a model dimension of 32 and a feed-forward dimension four times that of the embedding dimension. We extract the last token of the sequence as a 32-dimensional embedding for classification, followed by a dense layer with 2048 neurons and another dense layer corresponding to the number of categories. The input goes through an embedding layer that converts discrete tokens into a 32-dimensional vector. The input vocabularies are 256 for text and image and 16 for ListOps. The context lengths are 2048, 3072, and 1999 tokens, respectively, with 2, 10, and 10 output categories. In our modified architecture, we introduce our waveletGPT module between each decoder layer, retaining half of the embedding dimensions as they are. For the other half, we use non-learnable kernels, increasing the kernel size from 2, 4, and 8 to 512 linearly for dimensions 16 to 32 while maintaining the causality assumption. This introduces highways that hierarchically process data at each embedding and Transformer decoder layer without adding parameters, similar to our approach for LLM. As shown in Table 2, we achieve notable gains across all three modalities, where even minor improvements are worth reporting. We significantly

Table 2: Performance on LRA tasks (Tay et al. (2020b)) as reported in Liu et al. (2024). Bold the best-performing model, and underlined indicates the second-best. We use a baseline architecture for all three datasets (Section 5) and modify intermediate embeddings by imposing a hierarchical structure. Non-transformer-based, modified attention-based or hybrid architectures are not reported.

Transformer Based Attention Models	ListOps	Text	Image
Transformer (Vaswani et al., 2017)	36.37	64.27	42.44
Local Attention (Tay et al., 2020b)	15.82	63.98	41.46
Linear Trans. (Katharopoulos et al., 2020)	16.13	<u>65.90</u>	42.34
Linformer (Wang et al., 2020)	35.70	53.94	38.56
Sparse Transformer (Child et al., 2019)	17.07	63.58	44.24
Performer (Choromanski et al., 2021)	18.01	65.40	42.77
Sinkhorn Transformer (Tay et al., 2020a)	33.67	61.20	41.23
Longformer (Beltagy et al., 2020)	35.63	64.02	40.83
BigBird (Zaheer et al., 2020)	36.05	64.02	40.83
Luna-256 (Ma et al., 2021)	37.25	65.78	47.86
Reformer (Kitaev et al., 2020)	37.27	56.10	38.07
<hr/>			
FNET (Lee-Thorp et al., 2022) Non-Causal	37.27	56.10	38.07
WavSPA – Ada Transformer (Zhuang et al., 2024) - Non-Causal	<u>55.40</u>	81.60	<u>55.58</u>
<hr/>			
Ours (GPT Baseline With Classification Head)	41.65	65.32	49.81
Ours (WaveletGPT With Classification Head)	57.5	<u>66.38</u>	59.81

outperform non-causal methods, such as (Zhuang et al., 2024), with nearly 2% improvement on ListOps and 4.5% on a much smaller architecture—ours has 32 dimensions and six layers compared to 128 dimensions and eight layers. We limit our comparison method for fairness only with vanilla Transformer architectures. We also compare two non-casual architectures incorporating signal processing-based ideas: FNET and WavSPA.³ Compared to non-causal FNet, our model significantly outperformed all three LRA tasks, achieving 20% improvement on ListOps and Image and 10% on text. The most notable gain is in the ListOps task, which involves modelling a hierarchical, tree-like structure of math operations, making our model particularly suitable. To the best of our knowledge Liu et al. (2024), this is the best result achieved by simple attention-based Transformer on LRA tasks.

6 CONCLUSION AND FUTURE WORK

We showcase the powerful incorporation of a core signal processing idea, namely wavelets, into large language model pre-training. By imposing a multi-scale structure onto every intermediate embedding, we achieve the same performance 40-60% faster than a baseline architecture. We achieve a substantial performance boost if we train for the same number of steps. Our method generalizes across three modalities: raw text, symbolic music, and raw audio, giving similar performance speedups.

7 ACKNOWLEDGEMENT

This work was supported by the Stanford Institute of Human-Centered AI (HAI) through a Google Cloud computing grant. The author is thankful to Prof. Dan Jurafsky for feedback and helpful discussions on the problem and its impact on the field. I am also thankful to the anonymous reviewers for various suggestions.

REFERENCES

Martín Abadi, Paul Barham, Jianmin Chen, Zhifeng Chen, Andy Davis, Jeffrey Dean, Matthieu Devin, Sanjay Ghemawat, Geoffrey Irving, Michael Isard, et al. {TensorFlow}: A system for

³We do not compare it with other sophisticated state space-based methods or complex architectural changes as it would have required further tuning to our method/ significant architectural changes rather than straightforward, simple tweaks to have a fair comparison.

-
- {Large-Scale} machine learning. In *12th USENIX symposium on operating systems design and implementation (OSDI 16)*, pp. 265–283, 2016.
- Nasir Ahmed, T. Natarajan, and Kamisetty R Rao. Discrete cosine transform. *IEEE transactions on Computers*, 100(1):90–93, 1974.
- Rami Al-Rfou, Dokook Choe, Noah Constant, Mandy Guo, and Llion Jones. Character-level language modeling with deeper self-attention. In *Proceedings of the AAAI conference on artificial intelligence*, volume 33, pp. 3159–3166, 2019.
- Iz Beltagy, Matthew E. Peters, and Arman Cohan. Longformer: The long-document transformer. In *Proceedings of the 2020 Conference on Empirical Methods in Natural Language Processing (EMNLP)*, pp. 6150–6160, 2020. URL <https://www.aclweb.org/anthology/2020.emnlp-main.519/>.
- Zalán Borsos, Raphaël Marinier, Damien Vincent, Eugene Kharitonov, Olivier Pietquin, Matt Sharifi, Dominik Roblek, Olivier Teboul, David Grangier, Marco Tagliasacchi, et al. Audioldm: a language modeling approach to audio generation. *IEEE/ACM Transactions on Audio, Speech, and Language Processing*, 2023.
- Anthony Brohan, Noah Brown, Justice Carbajal, Yevgen Chebotar, Xi Chen, Krzysztof Choromanski, Tianli Ding, Danny Driess, Avinava Dubey, Chelsea Finn, et al. Rt-2: Vision-language-action models transfer web knowledge to robotic control. *arXiv preprint arXiv:2307.15818*, 2023a.
- Anthony Brohan, Noah Brown, Justice Carbajal, Yevgen Chebotar, Joseph Dabis, Chelsea Finn, Keerthana Gopalakrishnan, Karol Hausman, Alex Herzog, Jasmine Hsu, et al. Rt-1: Robotics transformer for real-world control at scale. In *Robotics: Science and Systems*. RSS, 2023b.
- T. Brown et al. Language models are few-shot learners. *arXiv preprint arXiv:2005.14165*, 2020.
- Charlotte Caucheteux, Alexandre Gramfort, and Jean-Rémi King. Evidence of a predictive coding hierarchy in the human brain listening to speech. *Nature human behaviour*, 7(3):430–441, 2023.
- Chameleon. Chameleon: Mixed-modal early-fusion foundation models. *arXiv preprint arXiv:2405.09818*, 2024. URL <https://arxiv.org/abs/2405.09818>.
- Rewon Child, Erich Elsen, David Kim, and Geoffrey Hinton. Sparse transformer. In *Proceedings of the 33rd Conference on Neural Information Processing Systems (NeurIPS 2019)*, 2019. URL <https://arxiv.org/abs/1904.10509>.
- Krzysztof Choromanski, Valerii Likhoshesterov, David Dohan, Xingyou Song, Andreea Gane, Tamas Sarlos, Peter Hawkins, Jared Davis, Afroz Mohiuddin, Lukasz Kaiser, David Belanger, Lucy Colwell, and Adrian Weller. Rethinking attention with performers. In *Proceedings of the 9th International Conference on Learning Representations (ICLR)*, 2021. URL <https://openreview.net/forum?id=Ua6zuk0WRH>.
- Alexandre Défossez, Jade Copet, Gabriel Synnaeve, and Yossi Adi. High fidelity neural audio compression. *arXiv preprint arXiv:2210.13438*, 2022.
- Tim Dettmers, Artidoro Pagnoni, Ari Holtzman, and Luke Zettlemoyer. Qlora: Efficient finetuning of quantized llms. *Advances in Neural Information Processing Systems*, 36, 2024.
- Jacob Devlin, Ming-Wei Chang, Kenton Lee, and Kristina Toutanova. Bert: Pre-training of deep bidirectional transformers for language understanding. In *Proceedings of the 2019 Conference of the North American Chapter of the Association for Computational Linguistics*, 2019.
- Alexey Dosovitskiy, Lucas Beyer, Alexander Kolesnikov, Dirk Weissenborn, Xiaohua Zhai, Thomas Unterthiner, Mostafa Dehghani, Horst Bischof, and Bernt Schiele. An image is worth 16x16 words: Transformers for image recognition at scale. In *Proceedings of the International Conference on Learning Representations (ICLR)*, 2021. URL <https://openreview.net/forum?id=Yg6M6i5Zx0>.

-
- William Fedus, Barret Zoph, and Noam Shazeer. Switch transformers: Scaling to trillion parameter models with simple and efficient sparsity. *Journal of Machine Learning Research*, 23(120):1–39, 2022.
- Fernando Flores-Mangas. Discrete wavelet transform. *The Washington Post*, Spring 2014. URL <https://www.cs.toronto.edu/~mangas/teaching/320/slides/CSC320L11.pdf>.
- E. Fonseca et. al. Fsd50k: an open dataset of human-labeled sound events. *arXiv preprint arXiv:2010.00475*, 2020.
- Robert X Gao and Ruqiang Yan. Non-stationary signal processing for bearing health monitoring. *International journal of manufacturing research*, 1(1):18–40, 2006.
- Karan Goel, Albert Gu, Chris Donahue, and Christopher Ré. It’s raw! audio generation with state-space models. In *International Conference on Machine Learning*, pp. 7616–7633. PMLR, 2022.
- Yuxian Gu, Li Dong, Furu Wei, and Minlie Huang. MiniLLM: Knowledge distillation of large language models. In *The Twelfth International Conference on Learning Representations*, 2024. URL <https://openreview.net/forum?id=5h0qf7IBZZ>.
- Curtis Hawthorne, Andriy Stasyuk, Adam Roberts, Ian Simon, Cheng-Zhi Anna Huang, Sander Dieleman, Erich Elsen, Jesse Engel, and Douglas Eck. Enabling factorized piano music modeling and generation with the maestro dataset. In *Proceedings of the International Conference on Learning Representations (ICLR)*, 2019. URL <https://openreview.net/forum?id=H1gJq2R5K7>.
- K. He et. al. Deep residual learning for image recognition. In *Proceedings of the IEEE conference on computer vision and pattern recognition*, pp. 770, 2016.
- Geoffrey Hinton, Oriol Vinyals, and Jeffrey Dean. Distilling the knowledge in a neural network. *arXiv preprint arXiv:1503.02531*, abs/1503.02531, 2015. URL <http://arxiv.org/abs/1503.02531>.
- Cheng-Zhi Anna Huang, Ashish Vaswani, Jakob Uszkoreit, Noam Shazeer, Ian Simon, Curtis Hawthorne, Andrew M Dai, Matthew D Hoffman, Monica Dinulescu, and Douglas Eck. Music transformer: Generating music with long-term structure. In *International Conference on Learning Representations (ICLR)*, 2019. URL <https://openreview.net/forum?id=rJe4ShAcF7>.
- Ke Huang and Selin Aviyente. Wavelet feature selection for image classification. *IEEE Transactions on Image Processing*, 17(9):1709–1720, 2008.
- Angelos Katharopoulos, Apoorv Vyas, Nikolaos Pappas, and François Fleuret. Transformers are rnns: Fast autoregressive transformers with linear attention. In *Proceedings of the 37th International Conference on Machine Learning (ICML)*, pp. 5156–5165. PMLR, 2020. URL <https://arxiv.org/abs/2006.16236>.
- Ruslan Khalitov, Tong Yu, Lei Cheng, and Zhirong Yang. Sparse factorization of square matrices with application to neural attention modeling. *Neural Networks*, 152:160–168, 2022.
- Nick Kingsbury and Julian Magarey. Wavelet transforms in image processing, 1998.
- Nikita Kitaev, Łukasz Kaiser, and Anselm Levskaya. Reformer: The efficient transformer. In *Proceedings of the 8th International Conference on Learning Representations (ICLR)*, 2020. URL <https://openreview.net/forum?id=rkgNkKhtvB>.
- Jan Koutník, Klaus Greff, Faustino Gomez, and Juergen Schmidhuber. A clockwork rnn. In *International conference on machine learning*, pp. 1863–1871. PMLR, 2014.

-
- James Lee-Thorp, Joshua Ainslie, Ilya Eckstein, and Santiago Ontanon. FNet: Mixing tokens with Fourier transforms. In Marine Carpuat, Marie-Catherine de Marneffe, and Ivan Vladimir Meza Ruiz (eds.), *Proceedings of the 2022 Conference of the North American Chapter of the Association for Computational Linguistics: Human Language Technologies*, pp. 4296–4313, Seattle, United States, July 2022. Association for Computational Linguistics. doi: 10.18653/v1/2022.naacl-main.319. URL <https://aclanthology.org/2022.naacl-main.319>.
- Zicheng Liu, Siyuan Li, Li Wang, Zedong Wang, Yunfan Liu, and Stan Z Li. Short-long convolutions help hardware-efficient linear attention to focus on long sequences. *arXiv preprint arXiv:2406.08128*, 2024.
- Jonathan Long, Evan Shelhamer, and Trevor Darrell. Fully convolutional networks for semantic segmentation. In *Proceedings of the IEEE conference on computer vision and pattern recognition*, pp. 3431–3440, 2015.
- Xuezhe Ma, Xiang Kong, Sinong Wang, Chunting Zhou, Jonathan May, Hao Ma, and Luke Zettlemoyer. Luna: Linear unified nested attention. In *Advances in Neural Information Processing Systems 34 (NeurIPS 2021)*, pp. 1235–1246, 2021. URL <https://proceedings.neurips.cc/paper/2021/hash/14319d9cfc6123106878dc20b94fbaf3-Abstract.html>.
- Andrew L. Maas, Raymond E. Daly, Peter T. Pham, Dan Huang, Andrew Y. Ng, and Christopher Potts. Learning word vectors for sentiment analysis. In *Proceedings of the 49th Annual Meeting of the Association for Computational Linguistics: Human Language Technologies*, pp. 142–150, Portland, Oregon, USA, June 2011. Association for Computational Linguistics. URL <http://www.aclweb.org/anthology/P11-1015>.
- Ali Madani, Bryan McCann, Nikhil Naik, Nitish Shirish Keskar, Namrata Anand, Raphael R Eguchi, Po-Ssu Huang, and Richard Socher. Progen: Language modeling for protein generation. *NeurIPS workshop on ML For Structural Biology*, 2020.
- Tomáš Mikolov, Ilya Sutskever, Anoop Deoras, Hai-Son Le, Stefan Kombrink, and Jan Cernocky. Subword language modeling with neural networks. *preprint (http://www.fit.vutbr.cz/imikolov/rnnlm/char.pdf)*, 8(67), 2012.
- Piotr Nawrot, Szymon Tworkowski, Michał Tyrolski, Lukasz Kaiser, Yuhuai Wu, Christian Szegedy, and Henryk Michalewski. Hierarchical transformers are more efficient language models. In Marine Carpuat, Marie-Catherine de Marneffe, and Ivan Vladimir Meza Ruiz (eds.), *Findings of the Association for Computational Linguistics: NAACL 2022*, pp. 1559–1571, Seattle, United States, July 2022. Association for Computational Linguistics. doi: 10.18653/v1/2022.findings-naacl.117. URL <https://aclanthology.org/2022.findings-naacl.117>.
- Naomi Nix. Silicon valley is pricing academics out of ai research. *The Washington Post*, March 2024. URL <https://www.washingtonpost.com/technology/2024/03/10/big-tech-companies-ai-research/>.
- papers-with code. Language modelling on text8. March 2024. URL <https://paperswithcode.com/sota/language-modelling-on-text8>.
- Javier Selva, Anders S Johansen, Sergio Escalera, Kamal Nasrollahi, Thomas B Moeslund, and Albert Clapés. Video transformers: A survey. *IEEE Transactions on Pattern Analysis and Machine Intelligence*, 2023.
- Mingjie Sun, Zhuang Liu, Anna Bair, and J Zico Kolter. A simple and effective pruning approach for large language models. In *The Twelfth International Conference on Learning Representations*, 2024. URL <https://openreview.net/forum?id=PxoFut3dWW>.
- A. Tamkin et. al. Language through a prism: A spectral approach for multiscale language representations. *Advances in Neural Information Processing Systems*, 33, 2020.
- Yi Tay, Donald Metzler, Xin Zhao, and Shuaiqiang Zheng. Sinkhorn transformer: Generating long-form text via randomized greedy sorting. In *Proceedings of the 37th International Conference on Machine Learning (ICML)*, pp. 9408–9419, 2020a. URL <http://proceedings.mlr.press/v119/tay20a.html>.

-
- Yi Tay, Mostafa Dehghani, Samira Abnar, Yikang Shen, Dara Bahri, Philip Pham, Jinfeng Rao, Liu Yang, Sebastian Ruder, and Donald Metzler. Long range arena : A benchmark for efficient transformers. In *International Conference on Learning Representations*, 2021. URL <https://openreview.net/forum?id=qVyeW-grC2k>.
- Zhilin Tay, Mostafa Dehghani, Ashish Vaswani, Noam Shazeer, and Jakob Uszkoreit. Local attention. In *Proceedings of the International Conference on Learning Representations*, 2020b.
- Gemini Team, Rohan Anil, Sebastian Borgeaud, Yonghui Wu, Jean-Baptiste Alayrac, Jiahui Yu, Radu Soricut, Johan Schalkwyk, Andrew M Dai, Anja Hauth, et al. Gemini: a family of highly capable multimodal models. *arXiv preprint arXiv:2312.11805*, 2023.
- Hugo Touvron, Thibaut Lavril, Gautier Izacard, Xavier Martinet, Marie-Anne Lachaux, Timothée Lacroix, Baptiste Rozière, Naman Goyal, Eric Hambro, Faisal Azhar, et al. Llama: Open and efficient foundation language models. *arXiv preprint arXiv:2302.13971*, 2023.
- Ashish Vaswani, Noam Shazeer, Niki Parmar, Jakob Uszkoreit, Llion Jones, Aidan N Gomez, Łukasz Kaiser, and Illia Polosukhin. Attention is all you need. In *Advances in neural information processing systems*, pp. 5998–6008, 2017.
- Prateek Verma. Goodbye wavenet—a language model for raw audio with context of 1/2 million samples. *arXiv preprint arXiv:2206.08297*, 2022.
- Prateek Verma and Jonathan Berger. Audio transformers: Transformer architectures for large scale audio understanding. *arXiv preprint arXiv:2105.00335*, 2021.
- Prateek Verma and Chris Chafe. A generative model for raw audio using transformer architectures. *2021 24th International Conference on Digital Audio Effects (DAFx)*, pp. 230–237, 2021. URL <https://api.semanticscholar.org/CorpusID:235683315>.
- Prateek Verma and Julius Smith. A framework for contrastive and generative learning of audio representations. *arXiv preprint arXiv:2010.11459*, 2020.
- Chengyi Wang, Sanyuan Chen, Yu Wu, Ziqiang Zhang, Long Zhou, Shujie Liu, Zhuo Chen, Yanqing Liu, Huaming Wang, Jinyu Li, et al. Neural codec language models are zero-shot text to speech synthesizers. *arXiv preprint arXiv:2301.02111*, 2023.
- Sinong Wang, Belinda Z. Li, Madian Khabsa, Han Fang, and Hao Ma. Linformer: Self-attention with linear complexity. *arXiv preprint arXiv:2006.04768*, 2020.
- Wilson Yan, Yunzhi Zhang, Pieter Abbeel, and Aravind Srinivas. Videogpt: Video generation using vq-vae and transformers. *arXiv preprint arXiv:2104.10157*, 2021.
- Lili Yu, Dániel Simig, Colin Flaherty, Armen Aghajanyan, Luke Zettlemoyer, and Mike Lewis. Megabyte: Predicting million-byte sequences with multiscale transformers. *Advances in Neural Information Processing Systems*, 36:78808–78823, 2023.
- Manzil Zaheer, Guru Guruganesh, Avinava Dubey, Joshua Ainslie, Chris Alberti, Santiago Ontanon, Philip Pham, Anirudh Ravula, Qifan Wang, Li Yang, and Amr Ahmed. Big bird: Transformers for longer sequences. In *Advances in Neural Information Processing Systems (NeurIPS)*, pp. 17283–17297, 2020. URL <https://proceedings.neurips.cc/paper/2020/hash/c8512d142a2d849725f31a9a7a361ab9-Abstract.html>.
- Yufan Zhuang, Zihan Wang, Fangbo Tao, and Jingbo Shang. Wavspa: Wavelet space attention for boosting transformers’ long sequence learning ability. In *Proceedings of UniReps: the First Workshop on Unifying Representations in Neural Models*, pp. 27–46. PMLR, 2024.

A REPRODUCIBILITY STATEMENT

We have included details of the dataset information and pre-processing pipelines, all publicly available to reproduce our results. Further, we have explained our algorithm, including all the necessary architectural information, learning rate schedules, algorithm details, training times, etc, to reproduce the results. Further, we will open-source our model code upon acceptance.

B ETHICS STATEMENT

No human subjects were used in this study. We aim to reduce the amount of time taken to pre-train an LLM. This paper is concerned with improving LLM pretraining and boosting its performance. So, all ethical concerns corresponding to large language models are identical. We do not open-source our code at this time but will do so upon acceptance of the paper.

C COMPARISON WITH EXPONENTIAL MOVING AVERAGES

We compare our method with Exponential Moving Averages (EMA) on the intermediate signals. This is widely used in time-series analysis for smoothening data, and it is another type of way that can modify intermediate signals. We proposed Haar wavelet, a multi-resolution kernel that can look at the input signal at various levels of scales depending on embedding dimension. We will now compare it against an EMA baseline and motivate where we differ and are similar to our proposed method.

C.1 BACKGROUND

Loosely speaking, instead of a moving average filter taking the mean of the signal, an EMA uses a different kernel, i.e., an exponential function. Meanwhile, a moving average kernel assigns equal weight to all time points. If we assume that the $x_i^l(t)$ signal of length is equal to context length after the l^{th} layer with t being the token index going from 0 to context length L at embedding dimension i , we can define the modified exponential smoothed version of the signal s_t as

$$s_0 = x_i^l(0) \quad s_t = \alpha x_i^l(t) + (1 - \alpha)s_{t-1}$$

Where α is the decay factor, it always satisfies $0 < \alpha < 1$. We can observe that for each of the tokens, depending on the decay factor α , we assign weights to the more recent values over the past values. When $\alpha = 1$, the weightage given is only to the current observation, and when $\alpha = 0$, it is just flat and gives equal weightage. The differences with moving average filters are evident, i.e., first, the moving average filter gives equal weight to all of the values in a window to update the values of a particular window. Depending on the value of α , an EMA filter gives an exponential weighted kernel. However, from the definition itself, an EMA filter, irrespective of the value of α , is an Infinite-Impulse response (IIR) filter. In contrast, a moving average filter is a finite impulse response (FIR) filter. Therefore, for every value update at a particular location, the values of dependencies of the previous samples will never be zero and relatively small. One can see that these values can add up significantly for some values of α when we are predicting the next tokens at longer context lengths. Due to the nature of the IIR filter, the values are never zero. They are assigned values weighed depending on the previous observation as $1, 1 - \alpha, (1 - \alpha)^2, (1 - \alpha)^3, \dots$

On the other hand, our proposed method includes wavelets composed mainly of FIR filters, including Haar or Daubechies. They are, therefore, only limited to a finite duration and can be adapted in multi-resolution setups with varied window lengths, as we have proposed in our paper. This allows us to have multi-scale information where we look at any signal at different resolutions with varied window lengths, with no contributions from components outside the desired window. (as we set the contribution from those values as 0). EMA, on the other hand, would still have some contribution from every component due to its recursive nature. One could also have a version similar to our method where one could vary α depending on the embedding dimension i . The update equations would now be a function of i , i.e.

$$s_0 = x_i^l(0) \quad s_t = \alpha_{(i)} x_i^l(t) + (1 - \alpha_{(i)})s_{t-1}$$

This would introduce different dimensions decaying at different rates. Even with varying decay rates, because of the inherent nature of the IIR filter, we still give weightage to all values, which are never zero, unlike the FIR filter, which utilizes a window and gives no weightage to values outside the window.

Training all possible values of α is beyond our scope and resources. We, therefore, give the best equivalent of the EMA algorithm with our proposed method, as described in the next section.

C.2 EXPERIMENTS AND RESULTS

We retain our baseline architecture precisely the same for text-8. We train for a context length of 512 with the same setup reported in our baseline section and the same dataset, with the only tweak being taking the baseline architecture and adding an EMA layer to it. We choose the number of decoder blocks to be 10, with 128 as the embedding dimension, the feed-forward dimension to be 512, and the number of heads to be 8. We opt for a two-layer feed-forward MLP inside the Transformer block after the attention block instead of a single layer typically used in Vaswani et al. (2017), with both the layers sharing the same number of neurons, i.e., 512, that of the feed-forward dimension. The final output layer of the Transformer decoder is then followed by a dense layer of 2048 neurons, followed by a dense layer of the same size as the vocabulary. This vocabulary size varies in the three modalities. For text8, it is 27, which is the number of characters plus an added extra token for space. Similar to our proposed method, we experiment with keeping half of the embedding dimensions in all the layers the same without any modifications. For the other half of the embedding dimension after all layers, we carry out EMA on 1-D signals, as described in the previous section, with α varying from 0 to 1 linearly for embedding dimensions 64 to 128. We see a drop in performance compared to our baseline architecture and achieve an NLL score of 0.94. For comparison, our baseline trained on text-8 scored 0.93, with our proposed method being 0.915 and 0.91 for learnable and non-learnable cases, respectively.

C.3 DISCUSSION

There can be many reasons why EMA degrades performance. One of them can be tuning α . There can be many possible choices, and tuning them for an expensive LLM pretraining is tough. Our proposed method, WaveletGPT, on the other hand, has a simple way of giving the weightage, which is grounded in signal processing and outperforms EMA smoothing. Further, in our learnable section, the architecture can learn the optimal **weights** in which, depending on the space spanned by the intermediate signals found inside LLM, it learns weights from scratch at different resolutions from the finest, i.e., window length 1 to the coarsest, i.e., window length as the context length 512.